Localization in an occupied-subspace-optimization approach to electronic structure: application to yttria-stabilized zirconia

David Raczkowski
NERSC, Lawrence Berkeley National Laboratory, Berkeley, CA 94720.

C.Y. Fong
Department of Physics, University of California, Davis, California 95616-8677

E.B. Stechel
Scientific Research Laboratories, Ford Motor Co., Dearborn, Michigan 48121-2053

Recently, we presented an occupied subspace optimization that replaces diagonalization in the serial gaussian density functional code SEQQUEST and commented on the accuracy of single point energies given a constraint of localization on the nonorthogonal Wannier-like orbitals that result. We now investigate the accuracy of calculations that involve relaxing the geometry of a system. The localization of these orbitals in our Gaussian representation gives asymptotic linear scaling of the computationally dominant terms.We analyze numerical aspects of the algorithm pertaining to the localization constraint on the orbitals. We focus on the effect of localization on the accuracy of the forces, relaxed geometries, relative energies, and formation enthalpies of Y_2O_3-stabilized ZrO_2 for system sizes up to 375 atoms.

PACS numbers:

I. Introduction

First-principles calculations have certainly impacted the role of computer simulations in materials science. Density functional theory (DFT) has proven to be a reliable tool for many materials of technological interest. Until recently, such computationally demanding DFT calculations were often constrained to very small systems of 1-10 atoms. Recent advances have made larger computations, involving ∼100 atoms, possible. For instance, the advent of massively parallel machines and codes that implement a real space mesh by use of Fourier transforms or finite-difference[1] coupled with iterative diagonalization[2] methods have allowed for simulations of much larger systems. The availability of these machines is limited, though. One common technique to bypass this limitation is the use of an atomic orbital[3]·[4] representation with the benefits of a comparatively small number of basis functions and resultant sparse matrices. The drawback of this method is the nonorthogonality of the basis, which prevents an easy prescription for adding more basis functions to increase the accuracy.

Another limitation is the $O(N^3)$ scaling of diagonalization in obtaining the electronic ground state. Linear Scaling algorithms[5][6][7][8][9] (for the purpose of this paper, any method utilizing localized Wannier-like occupied orbitals) have promise to be used as an alternative to diagonalization in DFT applications.[10][11][12]The effect of localization, restriction of the occupied orbitals to have a non-zero contribution from only selected basis functions (Gaussians in this paper), on scaling with system size and on accuracy of total energy has been studied predominantly with silicon and water clusters. The accuracy of localization and the corresponding computational effort for quantitative calculations need addressing in order to ascertain the usefulness of these algorithms as well as some familiarity of operational settings. Overall for linear scaling methods to become an integral part of the arsenal of the theoretical physicist, one needs to feel as comfortable with their reliability as exists with plane waves. This may be a task that may never be achieved, but for which at least strived. In Ref. [8], we investigated the effects of localization in determining relative energies between 3 polymorphs of SiC. In this paper, we now extend this investigation to the effect of localization on the accuracy of the forces, relaxed geometries, and formation enthalpies of YSZ, whose technological importance will be mentioned later.

For linear scaling techniques that employ an atomic orbital basis, one needs to establish the accuracy of the basis set for a particular problem. After this initial step, the rest of the paper addresses the effects of localization. The restriction of localization is an approximation that one needs to gain experience in using. A difficult step in using such an algorithm is determining *a priori* the required accuracy and the corresponding localization region for a calculation. One can either test a representative group of similar systems (ideally of small computational effort) that will give insight into the localization regions necessary for a larger calculation, or one can hope that one is using a large enough localization region. In this paper, we detail our tests on a representative group.

II. Occupied Subspace Optimization

Only a general overview of the algorithm is given. For a more detailed discussion the reader is referred to Ref [8]. For each self-consistent iteration, instead of solving the generalized eigenvalue equation,

$$\mathbf{H}\Psi=\mathbf{S}\Psi\mathbf{E}, \quad (1)$$

where Ψ is a M by N matrix of the coefficients of the M basis functions for the Noccupied eigenfunctions, the trace of a generalized Rayleigh quotient is minimized

$$\mathrm{Tr}[(\Phi^\dagger \mathbf{S}\Phi)^{-1}\ \Phi^\dagger \mathbf{H}\Phi\ ]. \quad (2)$$

The orbital matrix, Φ, is an M by N matrix of the coefficients for the N localized nonorthogonal occupied orbitals. We implement a Grassmann conjugate gradient algorithm[13] to minimize this trace. Typically, we use 15 conjugate gradient steps are per each self-consistent iteration. The algorithm accounts for the nonorthogonality of the basis and the occupied orbitals, which is necessary to obtain the gradient. This algorithm has been shown to approach a theoretical limit of convergence for a silicon system with no localization.[14]

In order to achieve linear scaling, each localized nonorthogonal orbital, a column of Φ, is restricted to have a non-zero contribution from only select basis functions. For this purpose, a localization radius is input for each shell of basis functions, e.g. the single zeta, double zeta, and polarization shells (see Ref. 8 for an in-depth discussion of shells). The accuracy increases as the localization radius increases, and is exact when the localization radius is greater than the size of the system. Using sparse matrix multiplies, the computationally dominant parts of the algorithm scale as O(N). At a certain system size (the crossover point), this method is more efficient than diagonalization.

We now address the sparsity of the other matrices. The sparsity pattern of the M x N matrices of the type $\mathbf{S}\Phi$ is determined in two ways. The first method is by input of a localization radius similarly as for Φ. In the second method, an element is kept if its value is above an input threshold value (growth parameter). The initial SCF cycle used the first method and subsequent cycles used the second method. The initial estimate of Φ was not sufficient for the second method to be used on the first SCF cycle. A growth parameter of $5\text{x}10^{-4}$ was generally observed to be sufficient for these calculations. For all results, the sparsity pattern was calculated and held fixed for each self-consistent field (SCF) cycle. For system sizes under 1000 atoms, the matrices $\Phi^\dagger \mathbf{H}\Phi$ and $\Phi^\dagger \mathbf{S}\Phi$ are not appreciably sparse; therefore, it is more efficient to use the appropriate dense machine-optimized routines.

III. Physical System and Basis Set Accuracy

YSZ exhibits high ionic conductivity and has found widespread use as electrolyte membranes in solid oxide fuel cells, oxygen pumps and separators, and other electrochemical devices.[15][16][17] Pure zirconia[18]·[19] (ZrO_2) exhibits three zero-pressure phases. The monoclinic phase is stable up to 1400 K, at which temperature it transforms into the tetragonal phase. At about 2650 K, this phase converts into the cubic fluorite structure. Yttria (Y_2O_3) assumes the bixbyite (a distorted fluorite lattice) structure.[20] Zirconia is stable in the fluorite phase at room temperature with approximately a 4-30 % moldoping of yttria. The Oxygen diffusion is at the highest around 8 % mol[21] of ytrria. We define one defect as $2\text{Zr} \rightarrow 2\text{Y}$ and an $\text{O} \rightarrow$ vacancy. Relaxation plays a major role in the relative energies; therefore, it is a good system to test the forces, ability to relax a complex system, and the relative energies for different localizations. For a thorough study of YSZ using plane waves see Ref. [22].

In order to test the accuracy of the basis set, we compare results with SEQQUEST[23] (DZP basis) using diagonalization against plane wave results as implemented in the VASP code[24] within the LDA approximation. Table I gives the relative energies of different phases of zirconia and yttria using both codes. For zirconia, we compare the monoclinic, tetragonal, and fluorite phases presented in increasing energy. For yttria, we compare the bixbyite and α-alumina phases. For both codes, we use **k**-point meshes of 4x4x4 for all zirconia phases and the α-alumina phase of yttria and a 2x2x2 for the bixbyite phase. The semicore p-states were kept in the valence for all cations. The plane wave results[22] use a 495 eV cutoff, and the energetics are in agreement with previous work.[18]·[19] The structural properties all lie within 1% of experiment for zirconia and yttria for both codes. The biggest discrepancy in the results of SEQQUEST is the relative energy of the monoclinic phase of zirconia. This is most likely attributable to the greater difference in atomic arrangement between the monoclinic and fluorite phases than between the tetragonal and fluorite phase. This discrepancy does suggest that comparing structures of significantly different atomic configurations might be problematic for LCAO basis sets. In our calculations with YSZ, we only investigate the cubic phase and have not encountered discrepancies of this magnitude.

We also compare the energetics of some composite YSZ structures by calculating the formation enthalpy ΔH, the (zero-pressure) energy difference between the YSZ compound, E(YSZ), and the composition-weighted average of its constituent oxides. With x the mole fraction of Y_2O_3, E_F the energy per ZrO_2 in the fluorite structure, and $E_B$energy per Y_2O_3 in the bixbyite structure, the formula is

$$\Delta\text{H} = \text{E(YSZ)} - [(1\text{-}x)(E_F) + x\ (E_B)\ ]. \quad (3)$$

In Table I, we show results for a $Zr_3Y_4O_{12}$ structure, the same stoichiometry (but probably not the same structure due to the positive formation energy) as the ordered compound[25] for YSZ. We also compare four $Zr_2Y_2O_7$ structures (see Ref[22] for specific information these structures). We chose these structures because they are small and span a variety of configurations and formation energies. All formation enthalpies are in good agreement. We did check the comparable accuracy with and without an Oxygen basis set on the vacancy site (ie. only the basis functions and not the actual ion). The difference in formation enthalpy is not significant, but in order to have uniformity in the functional space we chose to use the vacancy orbitals.

IV. Accuracy of Localization

We now investigate the accuracy of different localization regions compared to diagonalization using SEQQUEST.

A. Forces

Initially, we concentrate on the accuracy of the forces for different localization regions compared to diagonalization. We use a 24-atom unit cell obtained from doubling along each lattice vector of the 3 atom primitive cell of zirconia in the fluorite structure. This cell size is large enough to see localization effects, but small enough to be computationally fast. One yttria defect was inserted with the Y nearest neighbors (n.n.) to the vacancy. Due to the ionic nature of the compound, we chose to use atom-centered occupied orbitals as opposed to bond-centered. We centered four occupied orbitals on Oxygen and three on the cations. The initial guess for the Oxygen orbitals was strictly the single zeta s and p basis functions, and for the cations was the single zeta p.

In fig. 1, we compare the magnitude of the maximum error in the vector force difference of the forces obtained from the occupied subspace optimization with the forces from diagonalization at the initial geometry of the ideal fluorite crystal. For reference, the magnitude of the maximum force with diagonalization is 0.20467 Ry/Bohr at the ideal fluorite positions.

The horizontal axis is an approximate radius since the multiple radii for different basis functions prevent a pure definition of the localization radius. Even though we use a small **k**-point sampling, Γ point, for these calculations, it is acceptable as we are interested only in the comparison with diagonalization, which we also use only the Γ point. More **k**-points would give a more accurate charge density, but the differences in the self-consistent charge densities with different **k**-point meshes shouldn't change the localization properties. No significant difference in localization between a 24 and a 81 atom unit cell provides evidence for this statement.

From these results, we quickly obtain insight for acceptable settings of the localization radius. The localization region of the orbitals on the cations can be smaller as these are semi-core states. For the orbitals on the Oxygen atom, the inclusion of the polarization basis functions of the first nearest neighbor (n.n.) of Oxygen is crucial. The orbitals on the cations require either the single or double zeta of the first n.n. basis functions. One does not gain much in accuracy by increasing the orbitals on Oxygen if the orbitals on the cations have a small localization region, and vice versa.

B. Relaxation

Using the better localization settings obtained from the last section, we next check the accuracy of a geometry relaxation. We use an 81-atom with the configuration, labeled 1-A, of a single defect with both Y n.n. to the vacancy. The initial geometry is the ideal fluorite positions. The starting bond length was 4.15 Bohr. Fig 2 plots the magnitude of the maximum and rms of the vector difference of the final atomic positions vs. the approximate localization radius. Fig. 3 plots the same data for an 81-atom system with two Y_2O_3 defects. This configuration, labeled 2-A, has two vacancies separated by a Zr in the (111) direction (a distance denoted by (2;2;2)) and all Y n.n. to vacancies. A configuration is considered relaxed if the magnitude of the largest force on any atom is below $2\text{x}10^{-3}$ Ry/Bohr.

For the 2-A configuration, we encountered some problems relaxing if the vacancy orbitals are allowed to move. The vacancy orbitals started to move appreciably just before the relaxed geometry was achieved and the forces never reached convergence. If the vacancy orbitals are not allowed to move, a relaxed geometry is achieved. A localization region incorporating all Gaussian basis functions up the second n.n. for the Oxygen occupied orbitals and the first n.n. for the cations (radius of 5 Bohr for all orbitals) was necessary in order to relax this configuration.

C. Relative Energies and Formation Enthalpies

Finally, we compare the formation enthalpies of some 81-atom YSZ structures. For each system and defect configuration, we start from the ideal lattice, relax the atomic positions, and use the total energy at the final positions. In order for Eq. 3 to be consistent with the localization constraint, each of the energies in the equation must be calculated with the same localization region. From **k**-point calculations of the primitive unit cells, the Γ point is sufficiently converged for 192 (fluorite- ZrO_2) and 320 (bixbyite-Y_2O_3) atoms respectively and thus these systems were used to calculate E_F and E_B. Table II gives the formation enthalpy for diagonalization and for several localizations, given by approximate radius, for the 1-A configuration. The enthalpies do not approach the diagonalization value monotonically. This is not a breakdown of the variational principle, but a consequence of each of the energies in Eq. 3 monotonically decreasing at different rates.

In Table III, we give the formation enthalpies for several configurations with the localization radius of 5 Bohr for all orbitals. The new configurations are (1-B) – one defect with one Y n.n. to the vacancy; (2-B) – two vacancies as in 2-A and no Y n.n. to a vacancy; and (3) 2-C – two vacancies with more separation between them and no Y n.n. to a vacancy. The two vacancies in 2-C are still separated along the (111) direction, but now have 3 occupied FCC lattice between them, a distance of (4;4;4). For each configuration, we give the number of Y n.n. to a vacancy and the distance between the vacancies where applicable. The final row gives the formation enthalpies for the same configurations using diagonalization. The error from diagonalization is approximately the same for each configuration. This consistency is a reflection that

the relative energetics are correct. We get similar consistency for other localization regions also.

We chose these configurations in order to isolate a few interactions and find preferable positions between the constituents with only a few configurations. Most importantly, we wanted to test the accuracy for the localization for a few varied environments. The results have an overall consistency with previous plane wave calculations. We find the Y prefer not to be n.n. to the vacancy as do Ref [18, 22]. The preferred separation for the vacancies is not inconsistent with Ref[22], which found (2;2;2) to be optimal, as larger separation distances than (2;2;2) were not done. Recent diffuse scattering experiments[21] do suggest that the vacancies prefer to sit at the (2;2;2) distance but this is for higher defect concentrations where the larger separations may not be possible.

D. Computational Effort

With a localization radius of 5 Bohr for all orbitals (minimum necessary for relaxing all systems studied to the accuracy of 2x10^{-3} Ry/Bohr), the subspace optimization uses an approximately an equal amount (1Gb) of RAM memory as diagonalization for a system of 192 atoms. Using 15 conjugate gradient steps for 375 atoms, the occupied subspace optimization and diagonalization take approximately an equal amount of time (the crossover point) of 5,000 seconds. Similar number of self-consistent and relaxation steps were present for both diagonalization and the subspace optimization with this localization.

V. Summary

We have presented an investigation of the implementation of localization within an occupied subspace optimization for the quantitative analysis of a technologically important material, YSZ. We have established the accuracy of the Gaussian basis set. We utilized localization to produce linear scaling in the computationally dominant steps of the algorithm. The prominent results are the systematic study of the localization constraint (restriction of the occupied orbitals to have a non-zero contribution from only selected basis functions) on the nonorthogonal Wannier-like occupied orbitals. We concentrated on the effect on the accuracy of the forces, relaxed geometries, relative energies, and formation enthalpies of pure Zirconia and yttria, and the mixed compound of yttria-stabilized Zirconia (YSZ). The code has produced results comparable to plane wave results and capable of relaxation calculations of up to 375 atoms in 162 hours on a single DEC alpha 440 Mhz workstation.

Acknowledgements

Partial support was provided by the Campus Laboratory collaboration of the University of California and Sandia National Laboratories. Sandia is a multiprogram laboratory operated by Sandia Corporation, a Lockhead Martin Company, for the United States Department of Energy, under contract No. DEAC0494AL85000. C.Y. Fong acknowledges support from a NSF grant (no. Int-9872053). DBR acknowledges support and hospitality from Ford Motor Co. during the summer 1999. We gratefully acknowledge stimulating conversations with P. A. Schultz and A. Bogicevic, and great thanks to C. Wolverton for many helpful comments on the manuscript.

[1] James R. Chelikowsky, N. Troullier, and Y. Saad, Phys. Rev. Lett. **72**, 1240 (1994).
[2] M.C. Payne, M.P. Teter, D.C. Allan, T.A. Arias, and J.D. Joannopoulos, Rev. Mod. Phys. **64**, 1045 (1992)
[3] J. Almlöf and P.R. Taylor, Adv. Quantum Chem. **22**, 301 (1992)
[4] O.F. Sankey and D.J. Niklewski, Phys. Rev. B **40**, 3979 (1989)
[5] F. Mauri and G. Galli, Phys. Rev. B **50**, 4316 (1994).
[6] P. Ordejón, D. A. Drabold, R. M. Martin, et al., Phys. Rev. B **51**, 1456 (1995).
[7] E. B. Stechel, A. R. Williams, and P. J. Feibelman, Phys. Rev. B **49**, 10 088 (1994).
[8] D. Raczkowski, C.Y. Fong, P.A. Schultz, R.A. Lippert, and E.B. Stechel, in press
[9] X.-P. Li, R. W. Nunes, and D. Vanderbilt, Phys. Rev. B **47**, 10 891 (1993).
[10] P. Ordejón, Phys. Stat. Sol. (b) **217**, 335 (2000)
[11] G. E. Scuseria, J. Phys. Chem. A **103**, 4782 (1999)
[12] J. Bernholc, E.L. Briggs, C. Bungaro, M. Buongiorno Nardelli, J.-L. Fattebert, K. Rapcewicz, C. Roland, W.G. Schmidt, and Q. Zhao, phys, stat. Sol. (b) **217**, 685 (2000)
[13] A. Edelman, T. A. Arias, and S. T. Smith, SIAM J. on Matrix Anal. Appl. **20**, 303 (1998).
[14] R. A. Lippert and M. P. Sears, Phys. Rev. B **61**, 12 772 (2000).
[15] V.V. Kharton, A.A. Yaremchenko, and E.N. Naumovich, J. Solid Electrochem. **3**, 303(1999)
[16] A.J. Mcevoy, Solid State Ionics **132**, 159 (2000)
[17] T.H. Etsell and S.N. Flengas, Chem. Rev. **70**, 339 (1970).
[18] G. Stapper, M. Bernasconi, N. Nicoloso, and M. Parrinello, Phys. Rev. B **59**, 797 (1999).
[19] G. Jomard, T. Petit, A. Pasturel, et al., Phys. Rev. B **59**, 4044 (1999).
[20] B. H. O'Conner and T. M. Valentine, Acta Cryst. **B25**, 2140 (1969).
[21] J. P. Goff, W. Hayes, S. Hull, M.T. Hutchings, and K.N. Clausen, Phys. Rev. B **59**, 14 202 (1999).
[22] A. Bogicevic, C. Wolverton, G.M. Crosbie, and E.B. Stechel, Phys. Rev. B **64**, 014106 (2001).
[23] P. Schultz and P. J. Feibelman, to be published.

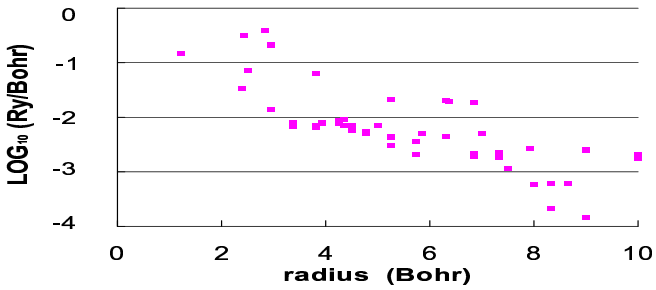

FIG. 1: Figure 1 For 24 atom zirconia unit cell with one defect, the maximum error in force vs. approximate localization radius.

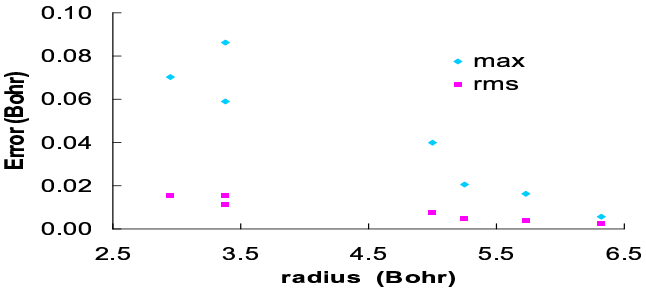

FIG. 2: Magnitude of the maximum and rms errors in final relaxed positions vs. approximate localization radius for configuration 1-A.

[24] G. Kresse and J. Hafner, Phys. Rev. B **47**, 558 (1993); **49**, 14 251 (1994).
[25] H.G. Scott, Acta Cryst. **B33**, 281 (1977)

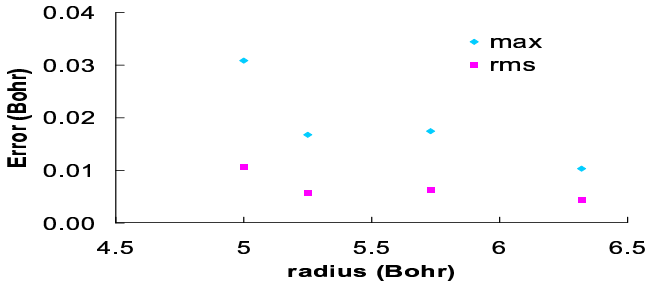

FIG. 3: Magnitude of the maximum and rms errors in final relaxed positions vs. approximate localization radius for configuration 2-A.

	VASP- Ref. 22	SEQQUEST- present
ZrO_2(T) – ZrO_2(F)	-36	-27
ZrO_2(M) – ZrO_2(F)	-81	-6
$Y_2O_3(\alpha)$ - Y_2O_3(B)	119	137
ΔH($Zr_3Y_4O_{12}$)	108	101
ΔH ($Zr_2Y_2O_7$–V2.a)	471	491
ΔH ($Zr_2Y_2O_7$–W2.a)	51	50
ΔH ($Zr_2Y_2O_7$–Y2.a)	121	114
ΔH ($Zr_2Y_2O_7$–Z2.a)	600	605

TABLE I: Table I. Relative energy differences between the monoclinic, tetragonal, and fluorite phases of ZrO_2, relative energy difference between the α-alumina and bixbyite phases of Y_2O_3, and formation enthalpy of YSZ structures in units of meV/cation.

	Diag	2.95	5	5.73	6.32	9
ΔH $Zr_{25}Y_2O_{53}$(1-A)	31.6	5.6	17.7	16.6	10.0	22.9

TABLE II: Table II. Formation enthalpy (meV/cation) for configuration 1-A for diagonalization and for several approximate localization radii.

	1-A	1-B	2-A	2-B	2-C
# Y-Vac NN pairs	2	1	ALL	NONE	NONE
Vac-Vac distance	—	—	2;2;2	2;2;2	4;4;4
5 radius	17.7	9.7	78.5	43.5	-13.9
diagonalization	31.6	24.2	95.2	58.6	-0.9

TABLE III: Table III. Comparison of formation enthalpy (meV/cation) for several configurations between diagonalization and a localization radius of exactly 5. Note, the distance given for 2-C is for the two vacancies in the same unit cell - the actual closest distance to any image is (4;2;2).